S1. Errors in GEOS-5 meteorological parameters

Errors in the GEOS-5 meteorology are quantified here using observational data from ISH and ISCCP. Results are exploited in Sect. 4 to evaluate the sensitivity of NO_2 columns simulated by GEOS-Chem to meteorological inputs.

To better understand the reliability of the meteorological fields, the analysis is conducted for a comprehensive set of parameters including air temperature, RH, tropospheric water vapor path, surface air pressure, 10m wind speed, cloud fraction, COD, and precipitation. Measurements are taken from the ISH dataset for air temperature, RH, surface air pressure, wind speed and precipitation, and are taken from ISCCP for tropospheric water vapor path, cloud fraction and COD. The analysis is emphasized in the daytime, particularly at mid-day when the lifetime of NOx is shortest and has the largest impact on its abundance at the overpass time of OMI (i.e., in the early afternoon).

S1.1 Air temperature

Surface (2m) air temperature in GEOS-5 differs from the NCDC ISH data (Fig. S1). In July, the GEOS-5 temperature at mid-day (mean over 0300-0600 UTC, or 11:00-14:00 Beijing local time (BLT)) is weakly correlated to the ISH data spatially, with an R^2 of 0.15. It is higher than ISH by up to 7 ℃ in the north (Fig. S1). Averaged over East China, the GEOS-5 temperature exceeds the ISH data by about 0.8 ℃ at 08:00-14:00 BLT but is about 1 ℃ lower at night (Fig. S1). The bias in daily mean is about -0.5 ℃ averaged over East China (Lin, 2012). For January, the spatial correlation between the two datasets increases significantly for mid-day temperature: the R^2 reaches 0.91. This is due mainly to the enhanced latitudinal temperature gradient from summer to winter captured by GEOS-5. Averaged over East China, GEOS-5 overestimates the ISH temperature by about 0.8 – 2.0 ℃ during the daytime and slightly underestimates it at night (Fig. S1). The temperature biases are caused in part by errors in cloud amount and COD (see Sect. S1.6) affecting the amount of radiation reaching the ground.

S1.2 Relative humidity

At mid-day, RH in the surface air (2m) also differs between GEOS-5 and ISH as a result of differences in air temperature and water vapor (Fig. S2). In July, the GEOS-5 RH is about 10-30% lower than ISH in the north but 10-30% higher in the south (Fig. S2). It is lower than

ISH at most stations in January (Fig. S2). The spatial correlation between GEOS-5 and ISH differs from that for air temperature: the R^2 increases to 0.46 in July and decreases to 0.32 for January. Diurnally, the GEOS-5 RH is lower than ISH during the daytime but is higher than ISH at night averaged over East China (Fig. S2).

S1.3 Tropospheric water vapor path

Measurements of water vapor path are taken from ISCCP with no information for diurnal variation. For daily mean values in July, the GEOS-5 dataset underestimates the water vapor path in ISCCP by more than 1 cm in the north, northwest, and southwest where the ISCCP values are normally lower than 5 cm (Fig. S3). It overestimates the ISCCP measurements in other regions with the ISCCP values exceeding 5 cm (Fig. S3). The R^2 for spatial correlation is about 0.63. Water vapor path decreases significantly from July to January, when the spatial variability in ISCCP is well captured by GEOS-5 resulting in a large R^2 of 0.77. In January, however, GEOS-5 underestimates the ISCCP water vapor path at most stations (Fig. S3).

S1.4 Surface air pressure

Day-to-day variation in surface air pressure is a good indicator of the large-scale circulation propagating through different regions of East China. The observed variation in ISH is reproduced by GEOS-5 with the R^2 close to unity in both January and July (Fig. S4), suggesting that the large-scale circulation is well constrained by the assimilation system. Meanwhile, the GEOS-5 data are in general lower than ISH with an average bias of about 10 hPa for East China in both months (Fig. S4). The bias decreases to about 2 hPa averaged over Northern East China (111.5°-122°E, 29°-41°N; Fig. S4), the main polluted region of China with a flatter terrain.

S1.5 Wind speed at 10m

Daily mean wind speed at 10m in GEOS-5 is normally much larger than ISH for both January and July, especially over regions of low wind speed (Fig. S5). Averaged over East China, the GEOS-5 wind speed is about 3.3 m/s in both months whereas the ISH winds are only about 2.4 – 2.5 m/s. The R^2 is less than 0.2 in both months for spatial correlation between GEOS-5 and ISH. The correlation is high between the two datasets for diurnal variation, with the R^2 reaching 0.68 in July and 0.86 in January.

S1.6 Cloud fraction and COD

The mid-day cloud fraction in GEOS-5 differs significantly from the ISCCP data (Fig. S6). In July, the GEOS-5 cloud fraction is lower than ISCCP by about 0.25 over most of East China but is slightly higher than ISCCP over the southern coastal regions. In January, GEOS-5 is about 0.1-0.25 lower than ISCCP in the north and the negative bias exceeds 0.5 in parts of the southern provinces. The correlation is low between the two datasets for both spatial and diurnal variations.

To evaluate the GEOS-5 COD, the in-cloud COD in ISCCP is converted to radiative mean COD taking into account the amount of cloud fraction (Liu et al., 2009). Correspondingly, the radiative mean COD for GEOS-5 is calculated as the sum over all tropospheric layers of the product of in-cloud COD and cloud fraction raised to the 1.5^{th} power assuming an approximate random overlap of clouds vertically (Liu et al., 2009). As with cloud fraction, the mid-day radiative mean COD derived from GEOS-5 differs significantly from that based on ISCCP (Fig. S7). In July, the GEOS-5 COD is lower than ISCCP by up to 5. In January, the negative biases exceed 5 in parts of the south and are less than 1.5 in the north. The relative (percentage) error exceeds 50% in most areas for both months. Spatially and diurnally, the correlation is low between the two datasets. The relative errors for daytime mean COD in GEOS-5 are similar to those at mid-day (not shown).

S1.7 Precipitation

On the regional mean basis, the amount of daily precipitation in GEOS-5 is consistent with ISH. In GEOS-5, daily precipitation exhibits significant seasonal variability, with a regional mean of 6.5 mm/day in July and 1.0 mm/day in January. Meanwhile, the regional mean for ISH is about 6.5 mm/day in July and 0.85 mm/day in January. Differences between GEOS-5 and ISH are larger at individual stations (Fig. S8). The R^2 is about 0.35 in July and 0.38 in January for spatial correlation between the two datasets.

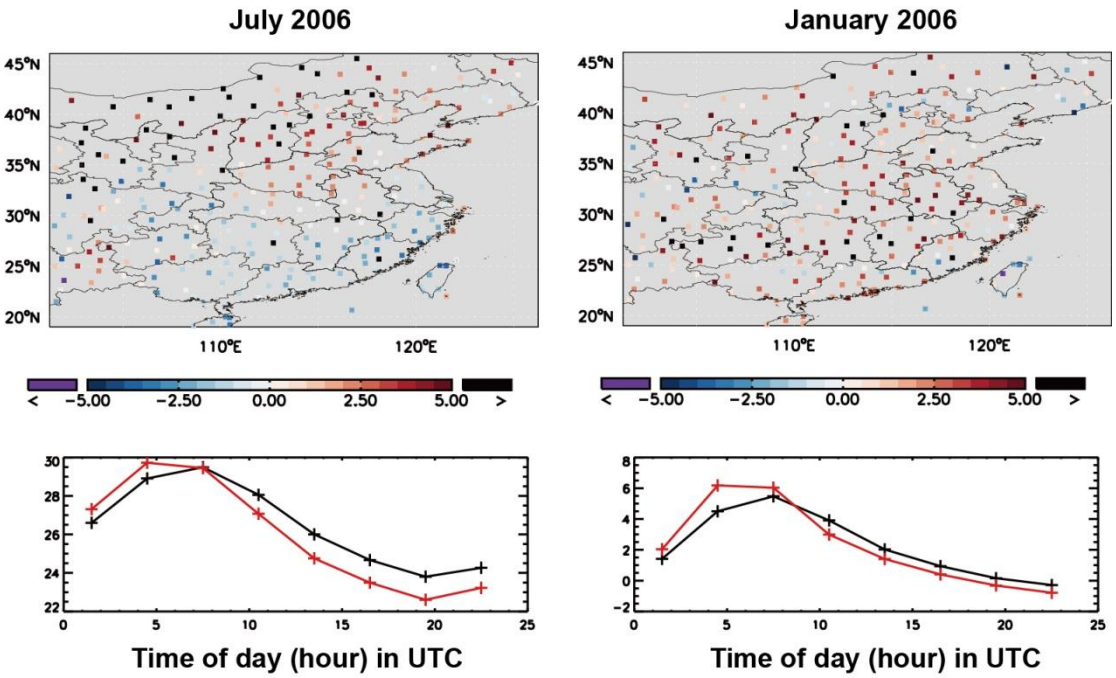

Fig. S1. (top) Differences (℃) between GEOS-5 and ISH in monthly mean near-surface air temperature at mid-day (11:00-14:00 BLT). (bottom) Diurnal variation of air temperature (℃) in ISH (black) and GEOS-5 (red) averaged over East China. Data are presented at three-hour intervals (0000-0300 UTC mean, 0300-0600 UTC mean, etc.).

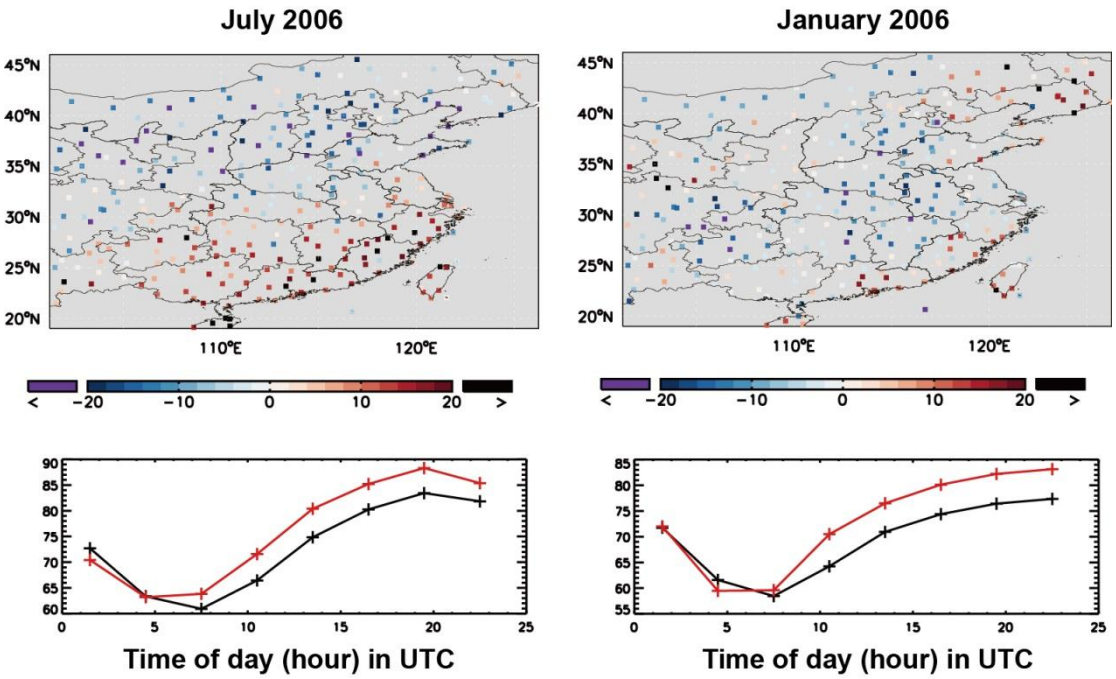

Fig. S2. Similar to Fig. S1 but for near-surface relative humidity (%).

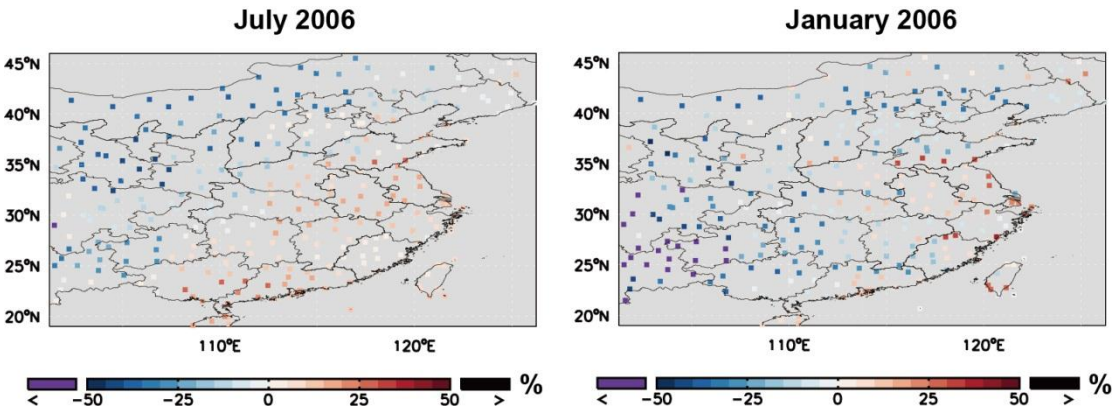

Fig. S3. (top) Percentage differences between GEOS-5 and ISCCP in monthly mean daily mean tropospheric water vapor path.

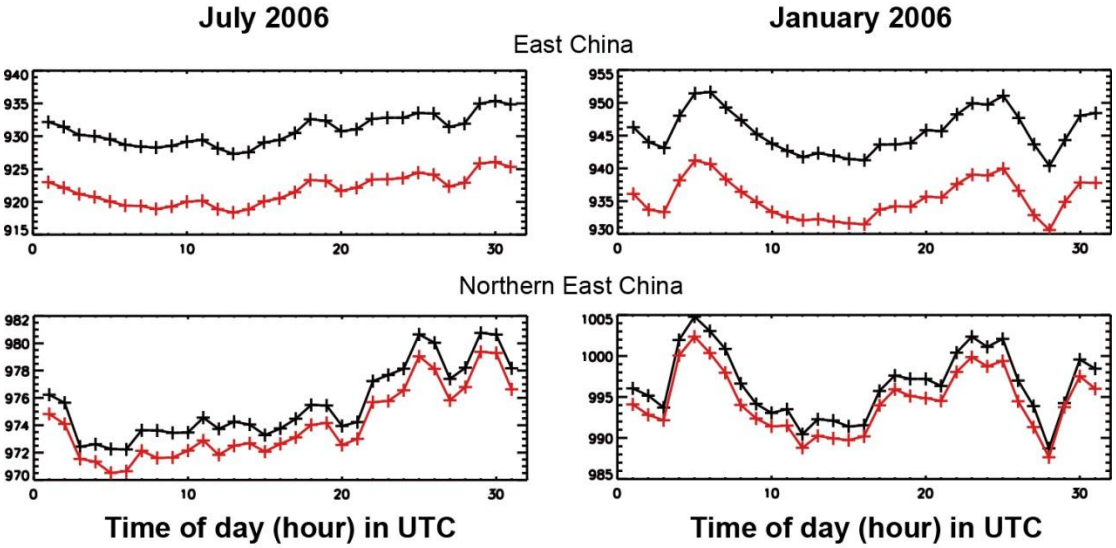

Fig. S4. Daily variation of surface air pressure in ISH (black) and GEOS-5 (red). Northern East China covers 111.5°-122°E and 29°-41°N.

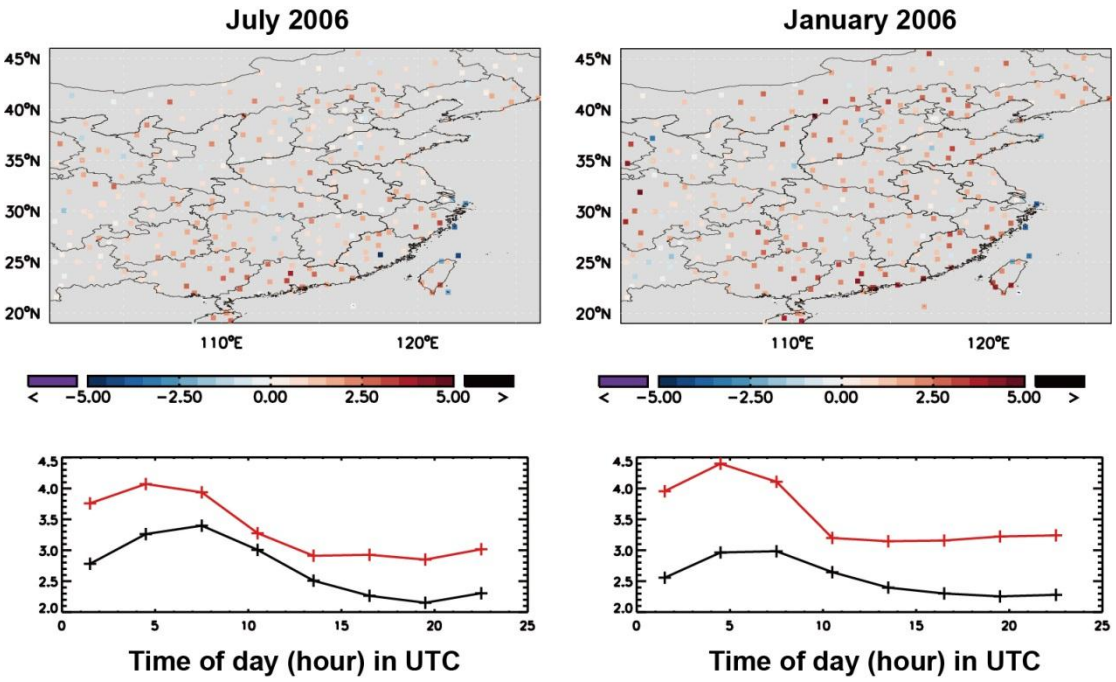

Fig. S5. (top) Differences (m s^{-1}) between GEOS-5 and ISH in monthly mean daily mean 10m wind speed. (bottom) Diurnal variation of wind speed (m s^{-1}) in ISH (black) and GEOS-5 (red) averaged over East China. Data are presented at three-hour intervals (0000-0300 UTC mean, 0300-0600 UTC mean, etc.).

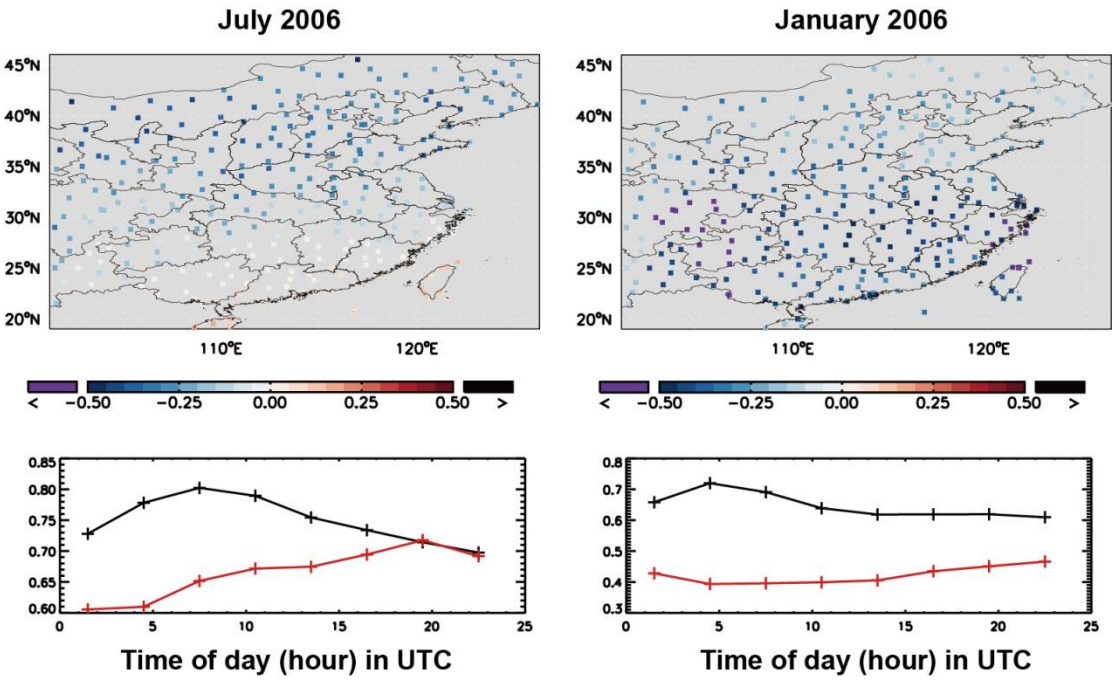

Fig. S6. Similar to Fig. S1 but for comparison of cloud fraction between GEOS-5 and ISCCP.

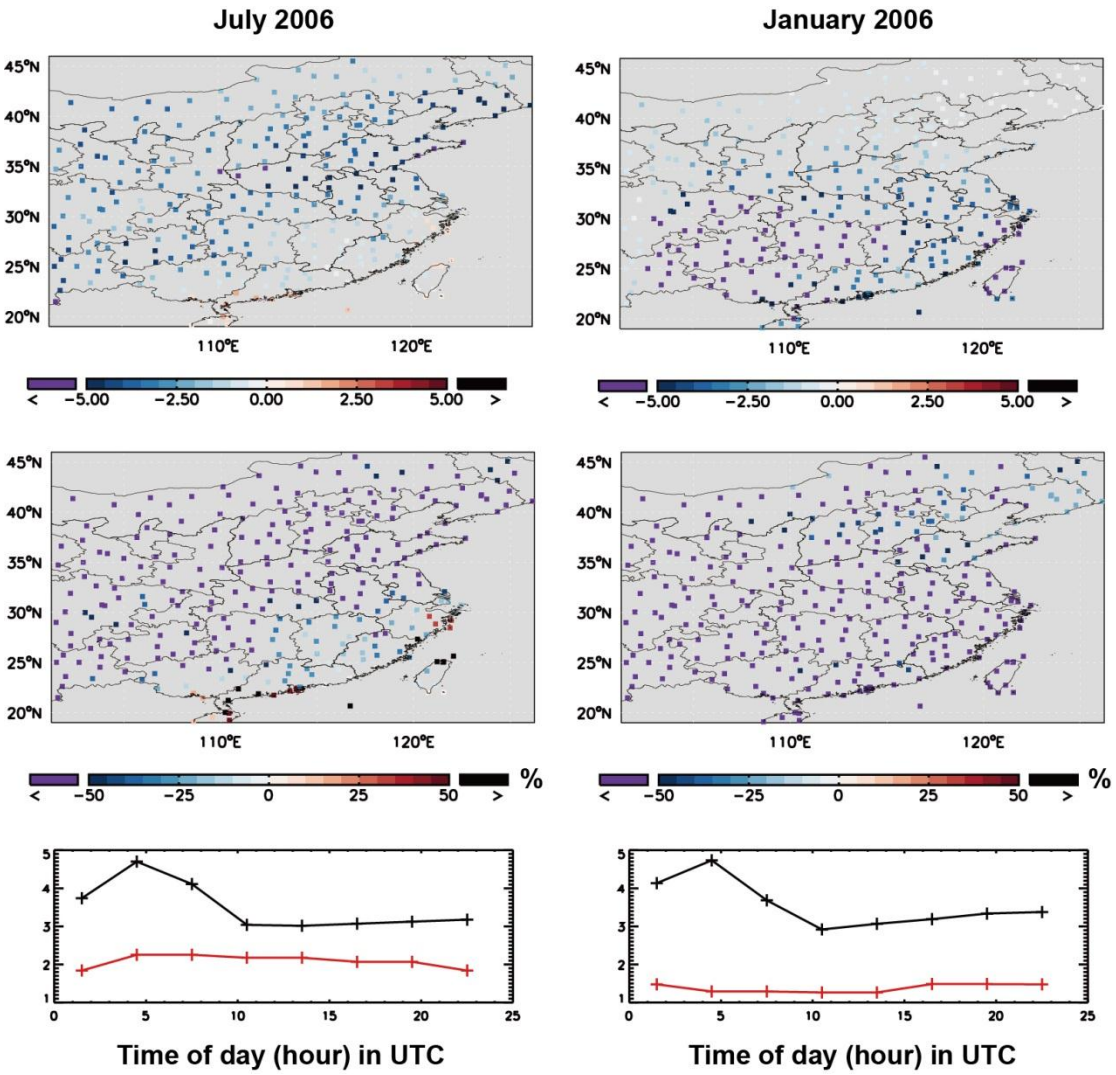

Fig. S7. (top) Differences between GEOS-5 and ISCCP in monthly mean radiative mean cloud optical depth at mid-day (11:00-14:00 BLT). (middle) The respective percentage differences. (bottom) Diurnal variation of radiative mean cloud optical depth in ISCCP (black) and GEOS-5 (red) averaged over East China. Data are presented at three-hour intervals (0000-0300 UTC mean, 0300-0600 UTC mean, etc.).

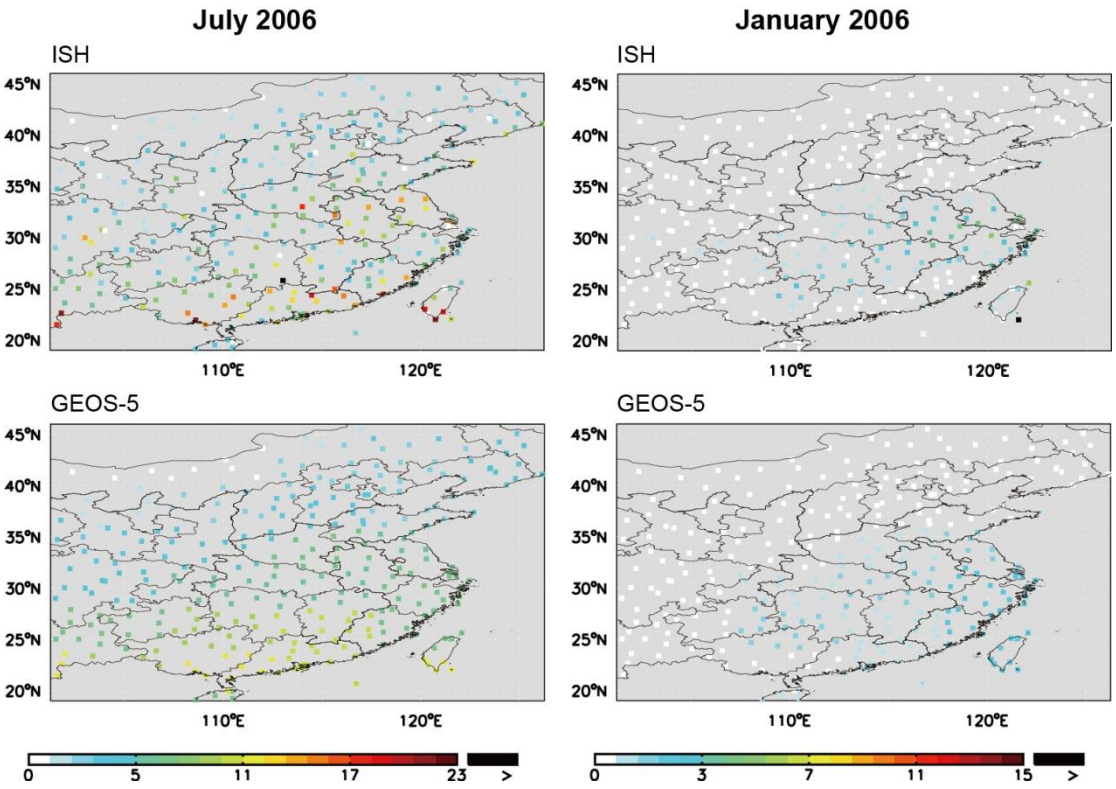

Fig. S8. Spatial distribution of monthly mean daily precipitation (mm d^{-1}) in ISH and GEOS-5.

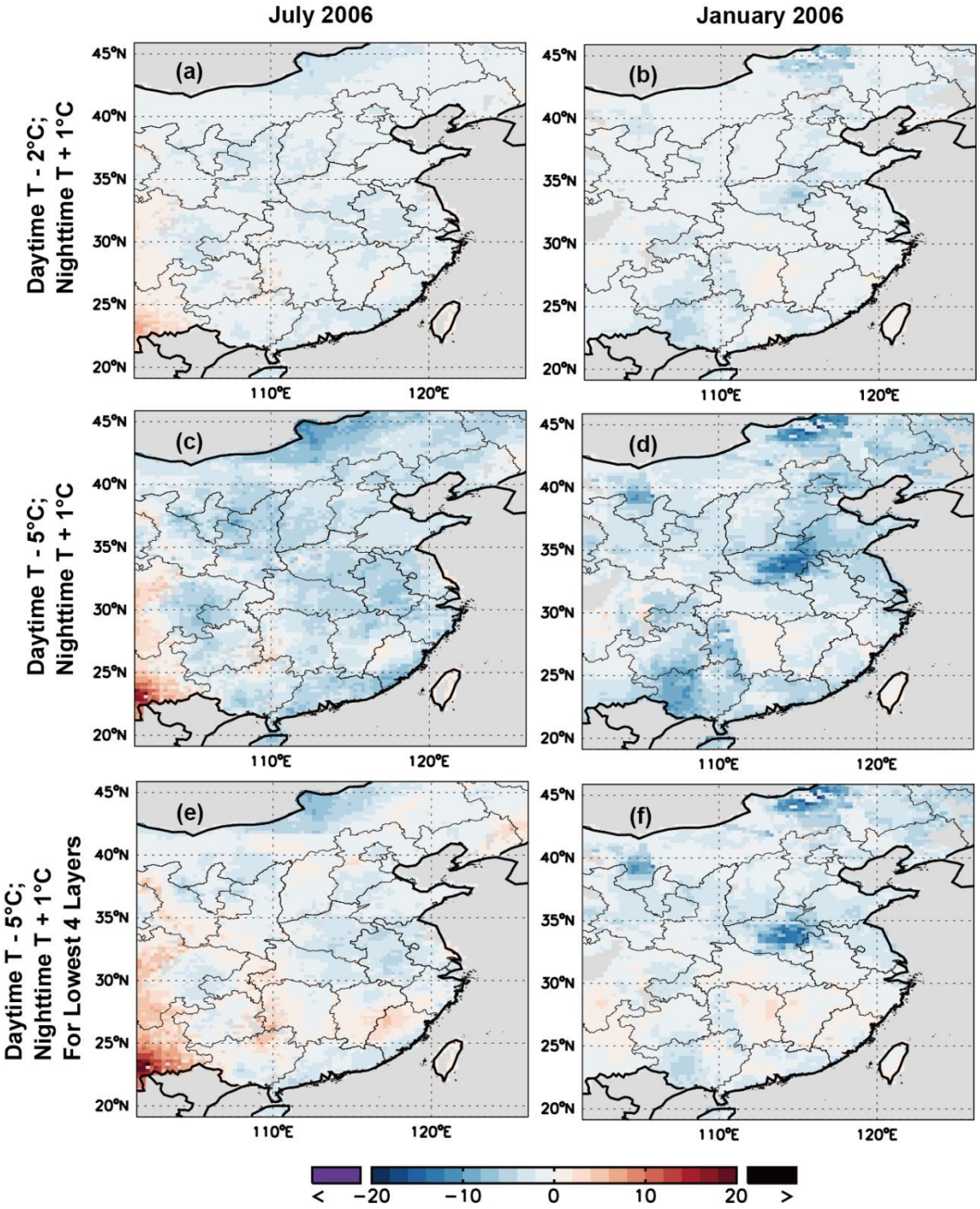

Fig. S9. Spatial distribution of percentage differences between modeled NO_2 columns with and without adjustments in air temperature. (a,b) The daytime temperature is decreased by 2 ℃ with an increase of 1 ℃ at night for the lowest 10 model layers. (c,d) The daytime temperature is decreased by 5 ℃ with an increase of 1 ℃ at night for the lowest 10 model layers. (e,f) The daytime temperature is decreased by 5 ℃ with an increase of 1 ℃ at night for the lowest four model layers. Panels (c,d) are the same as Fig. 3.

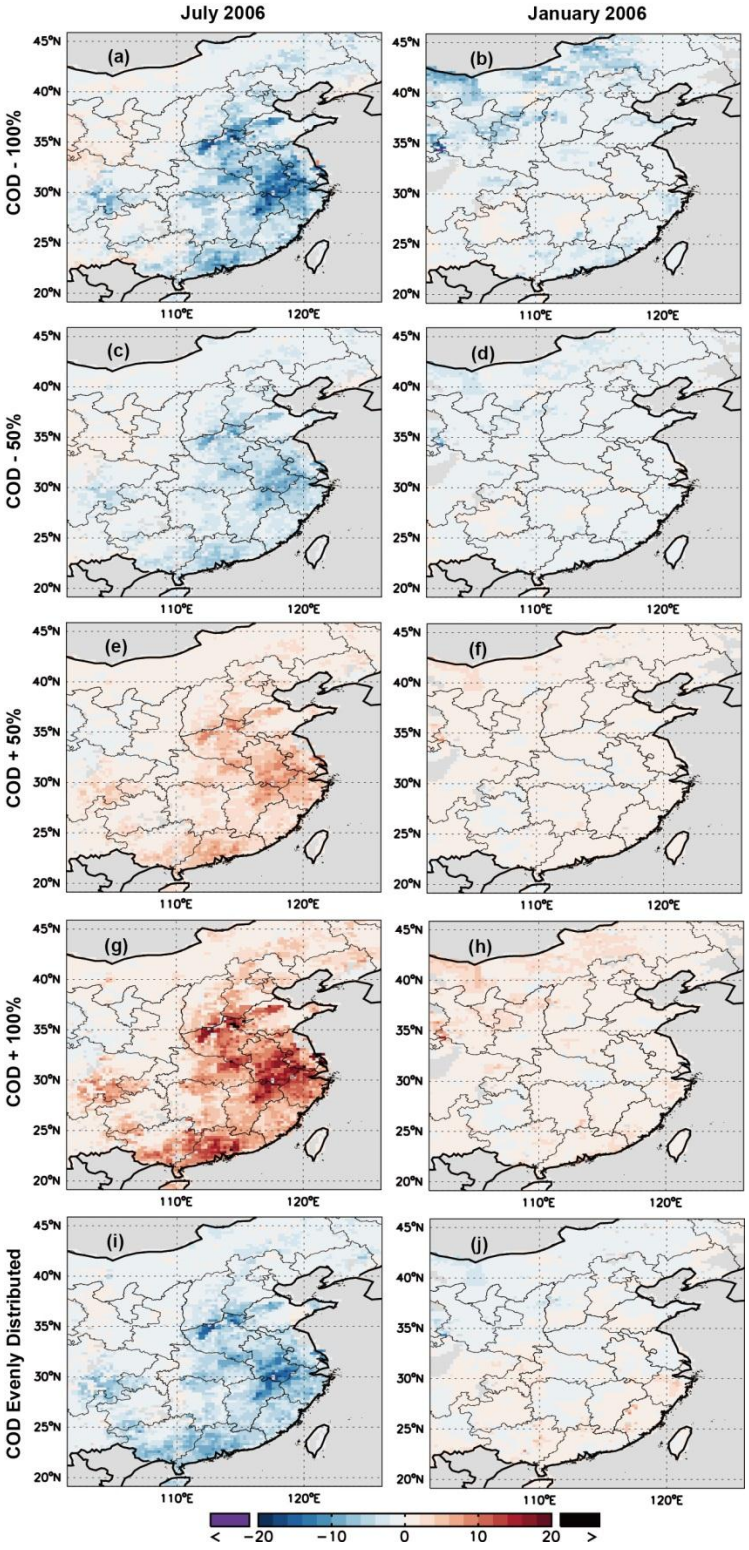

Fig. S10. Spatial distribution of percentage differences between modeled NO_2 columns with and without adjustments in COD. The COD is scaled by a factor of 0% (a,b), 50% (c,d), 150% (e,f) and 200% (g,h); or is assumed to be distributed evenly in all tropospheric layers (i,j). Panels (g,h) are the same as Fig. 5.

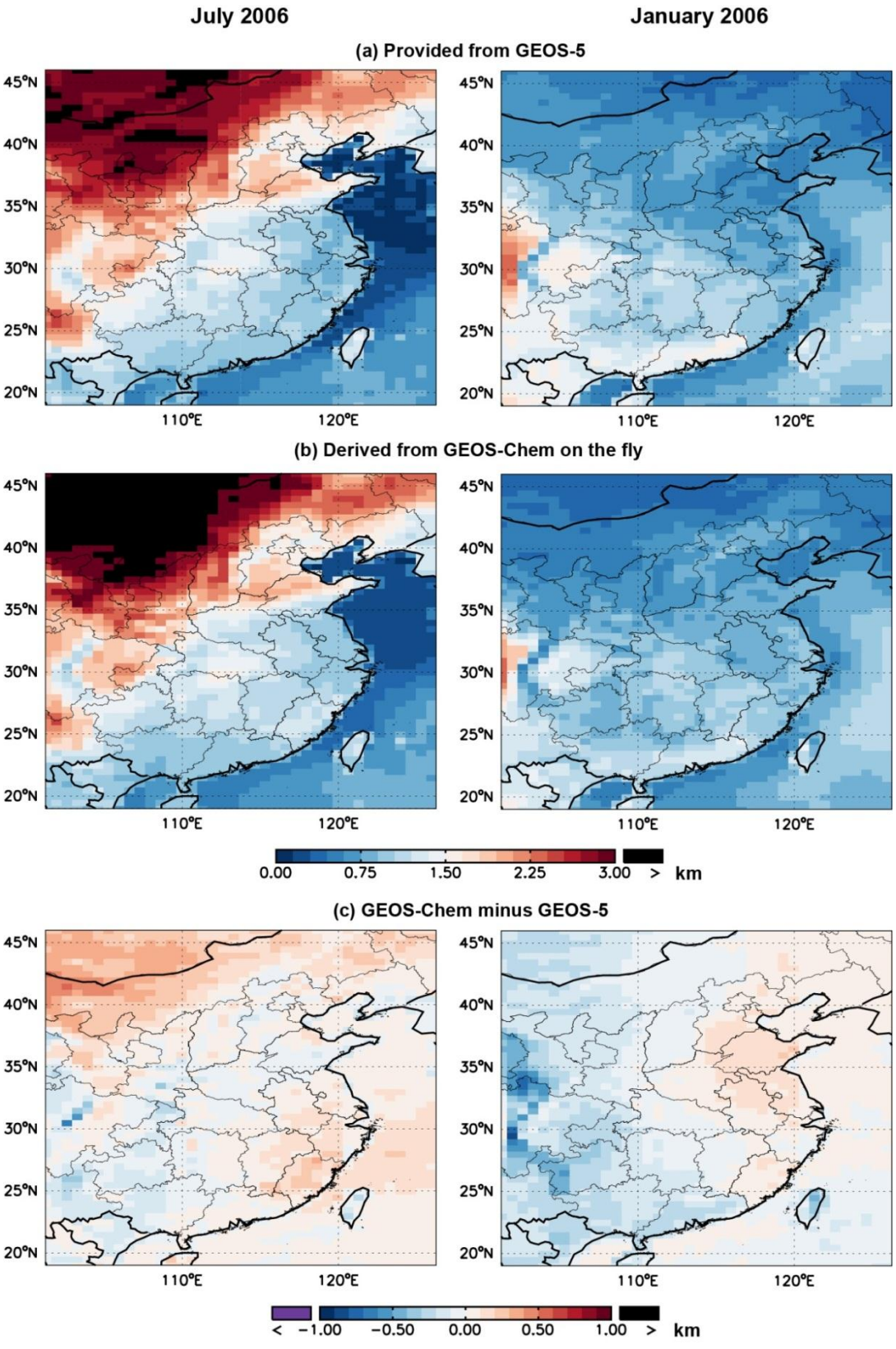

Fig. S11. The PBLH taken from GEOS-5 versus derived from GEOS-Chem online using a non-local scheme at 13:00-15:00 local time (i.e., around the overpass time of OMI).

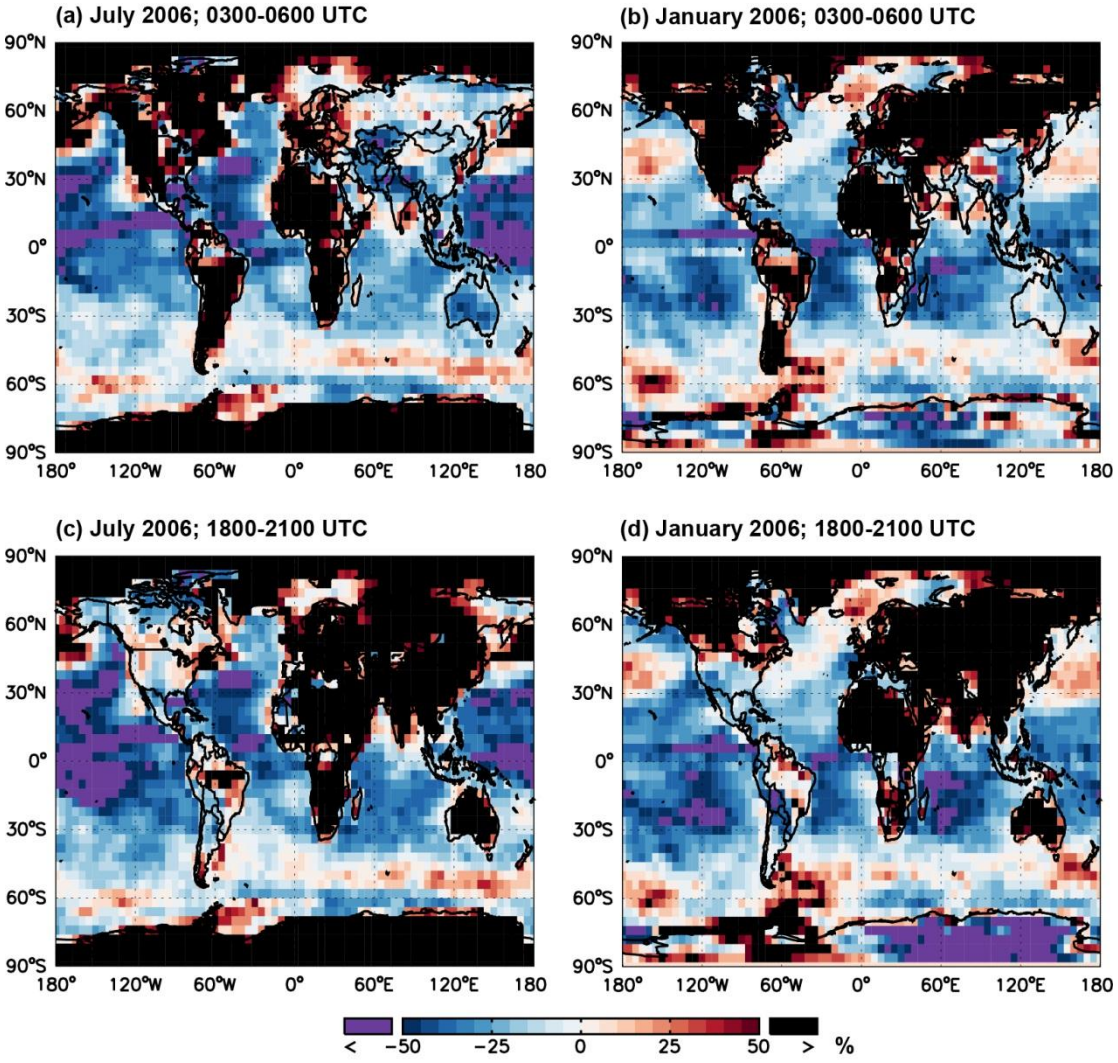

Fig. S12. Percentage differences of the GEOS-4 PBLH relative to GEOS-5 on the 2.5 °long x 2 °lat grid. The local time is around mid-day in Beijing and before mid-night in New York in (a,b); and is after mid-night in Beijing and in the early afternoon in New York in (c,d).

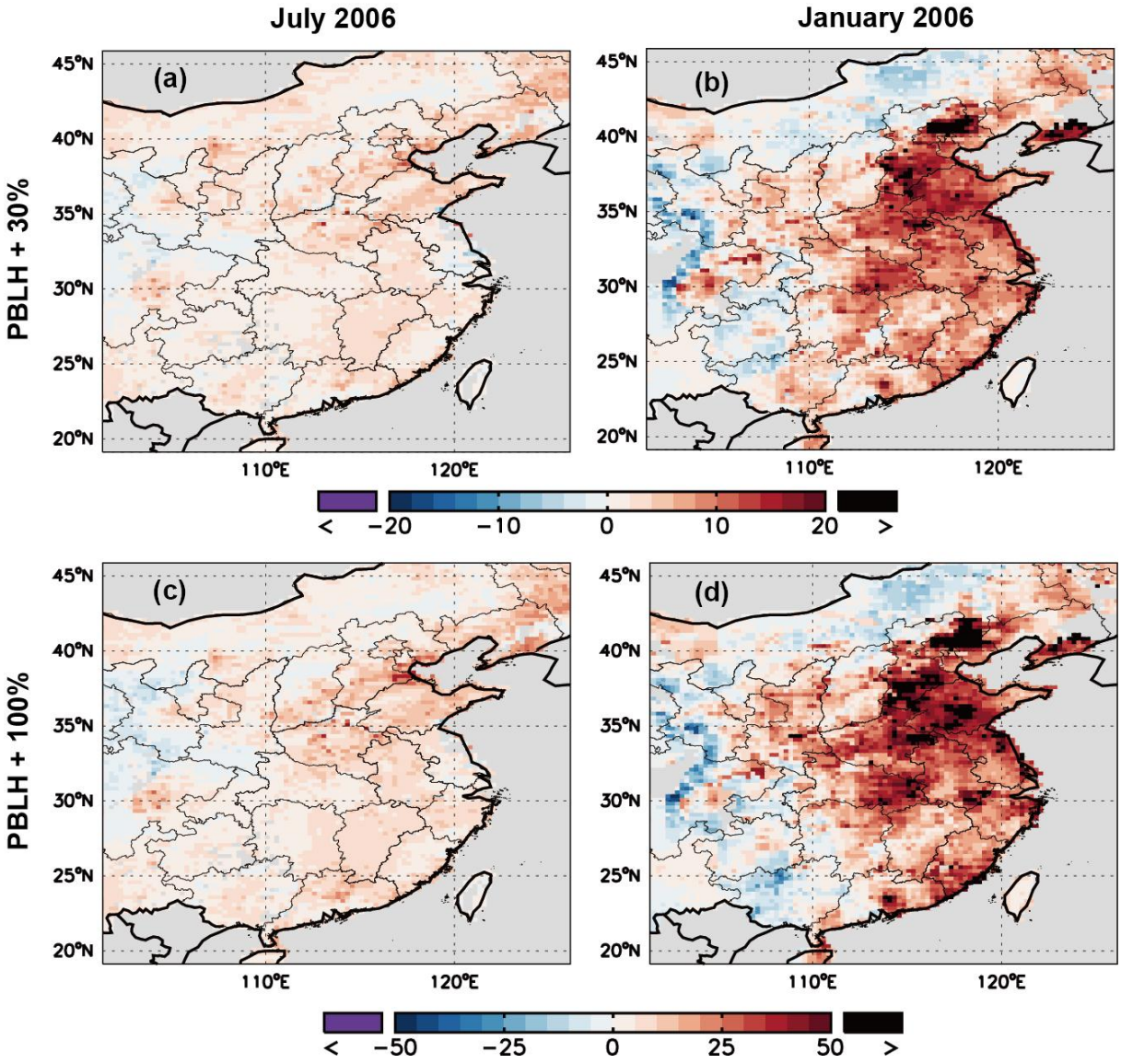

Fig. S13. Spatial distribution of percentage differences between modeled NO_2 columns with and without adjustments in PBLH. (a,b) The PBLH is increased by 30%. (c,d) The PBLH is increased by 100%.

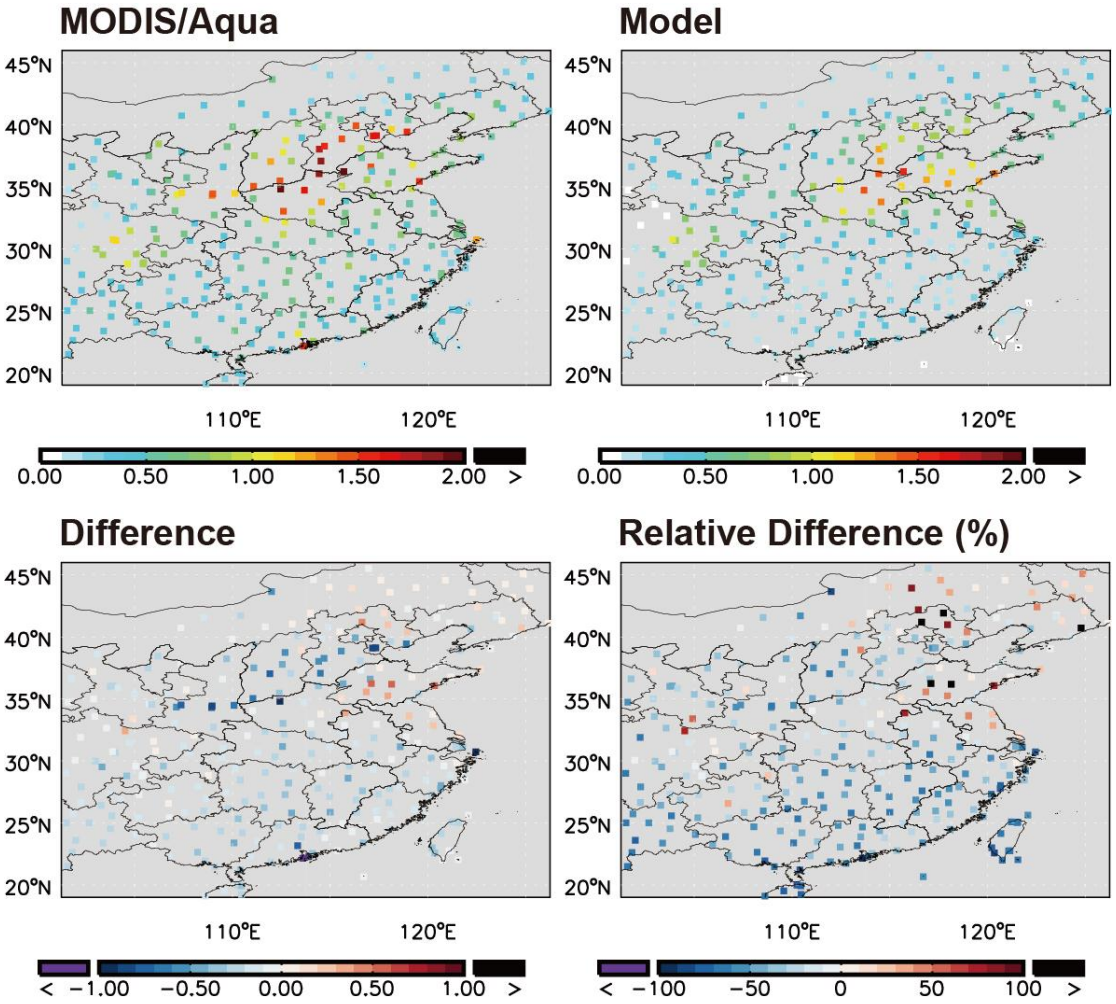

Fig. S14. July mean AOD in MODIS versus GEOS-Chem. Model values are sampled at 13:00-15:00 local time in days with valid MODIS data for a consistent comparison.

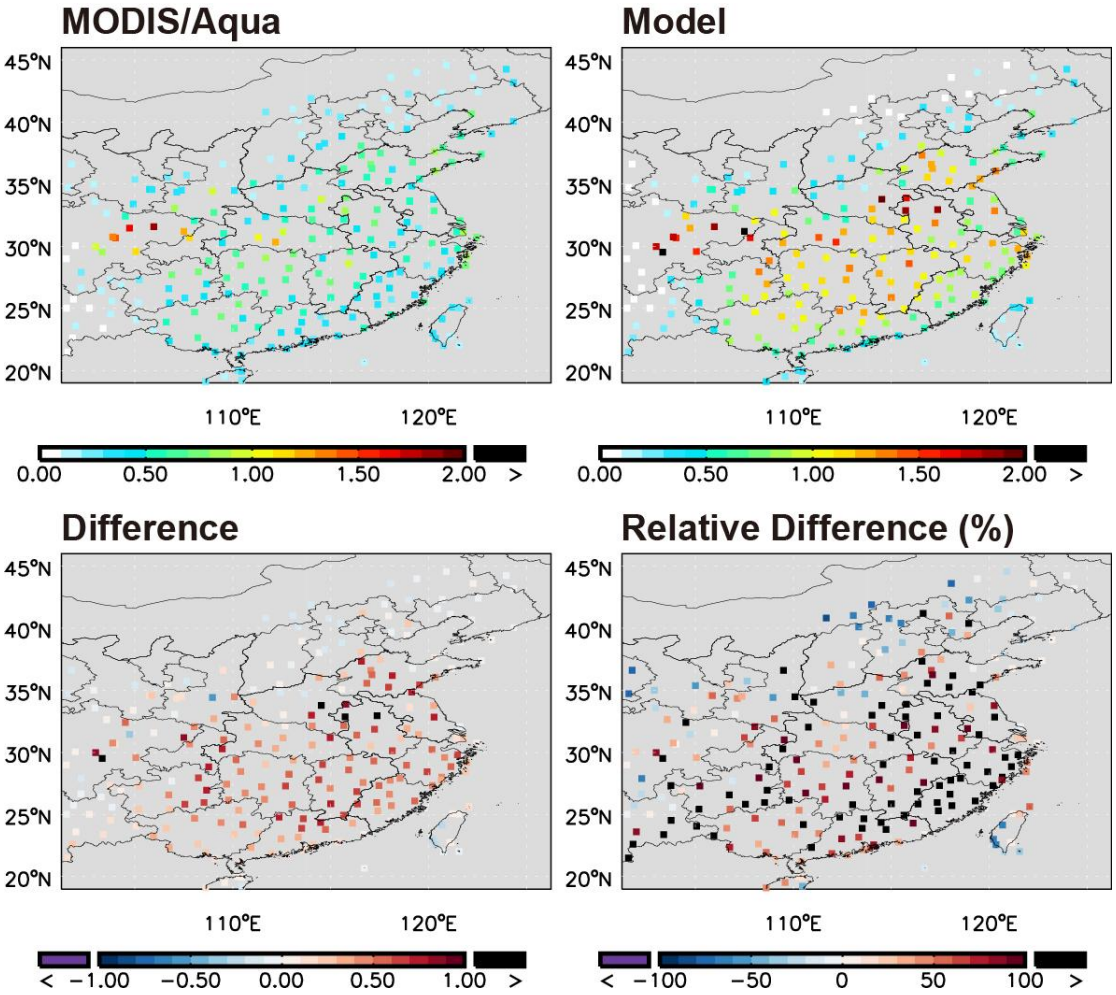

Fig. S15. Similar to Fig. S14 but for January 2006.

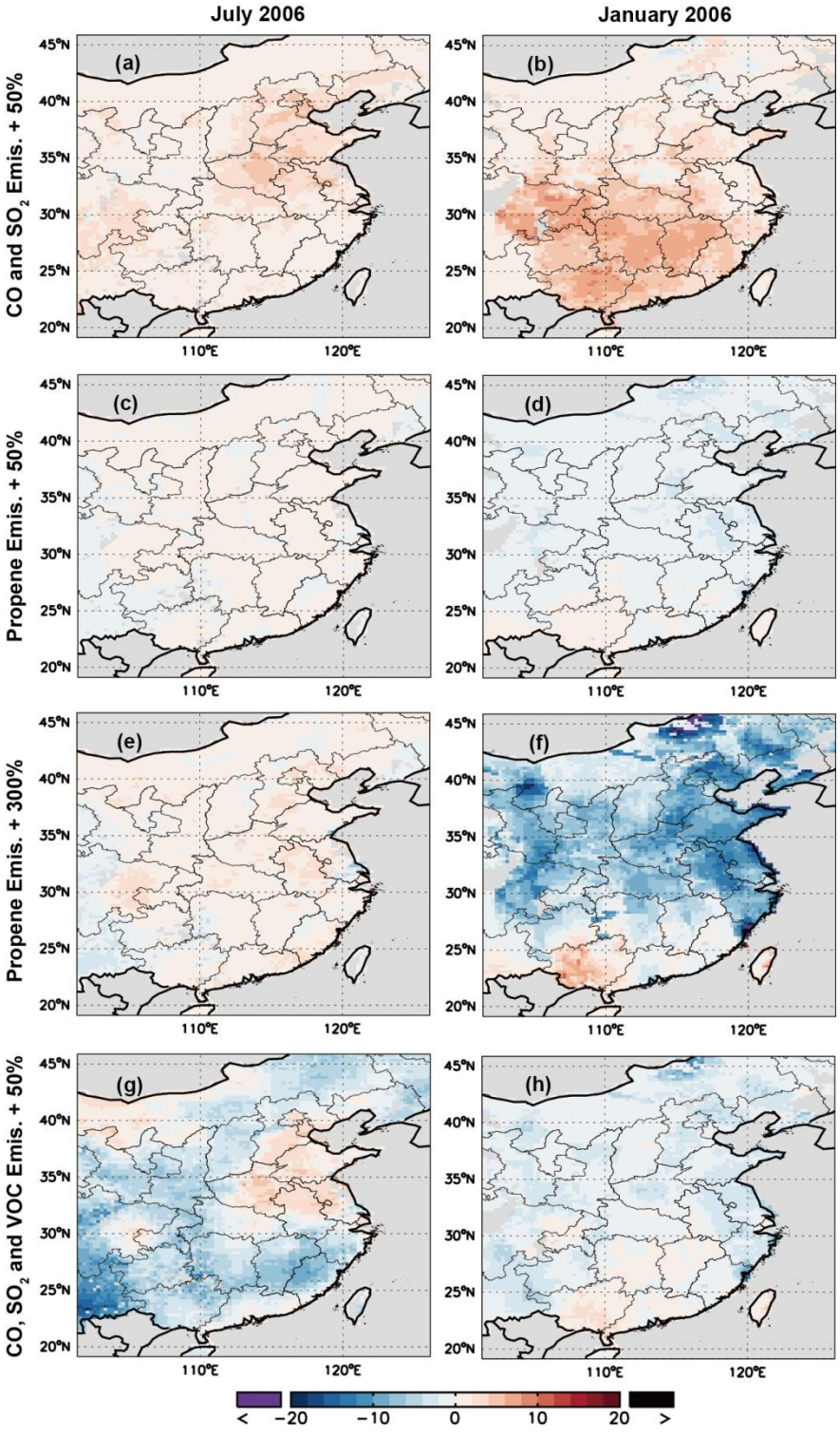

Fig. S16. Spatial distribution of percentage differences between modeled NO_2 columns with and without adjustments in emissions. (a,b) Emissions of CO and SO_2 are increased by 50%. (c,d) Emissions of propene are increased by 50%. (e,f) Emissions of propene are increased by 300%. (g,h) Emissions of CO, SO_2 and VOC are increased by 50%. Panels (e,f) are the same as Fig. 12.

References:

Lin, J.: Satellite constraint for emissions of nitrogen oxides from anthropogenic, lightning and soil sources over East China on a high-resolution grid, Atmos. Chem. Phys., 12, 2881-2898, doi: 10.5194/acp-12-2881-2012, 2012.

Liu, H., Crawford, J. H., Considine, D. B., Platnick, S., Norris, P. M., Duncan, B. N., Pierce, R. B., Gao, C., and Yantosca, R. M.: Sensitivity of photolysis frequencies and key tropospheric oxidants in a global model to cloud vertical distributions and optical properties, Journal of Geophysical Research, 114, D10305 (10317 pp.)-D10305 (10317 pp.)D10305 (10317 pp.), doi: 10.1029/2008jd011503, 2009.